ATION PAGE

Form Approved
OMB No. 0704-0188

1. AGENCY USE ONLY *(Leave blank)*	2. REPORT DATE	3. REPORT TYPE AND DATES COVERED
	March 1992	Professional Paper

4. TITLE AND SUBTITLE

EXTRACTION EFFICIENCY UNIFORMITY IN RARE GAS HALIDE LASERS

5. FUNDING NUMBERS

PR: ZE70
PE: 0602936N
WU: DN308067

6. AUTHOR(S)

R. Scheps

7. PERFORMING ORGANIZATION NAME(S) AND ADDRESS(ES)

Naval Command, Control and Ocean Surveillance Center (NCCOSC),
Research, Development, Test and Evaluation Division (NRaD)
San Diego, CA 92152-5000

8. PERFORMING ORGANIZATION REPORT NUMBER

9. SPONSORING/MONITORING AGENCY NAME(S) AND ADDRESS(ES)

Office of Chief of Naval Research
Independent Exploratory Development Programs (IED)
OCNR-20
Arlington, VA 22217

10. SPONSORING/MONITORING AGENCY REPORT NUMBER

11. SUPPLEMENTARY NOTES

12a. DISTRIBUTION/AVAILABILITY STATEMENT

Approved for public release; distribution is unlimited.

12b. DISTRIBUTION CODE

13. ABSTRACT *(Maximum 200 words)*

The dependence of the extraction efficiency on the temporal variations in the quenching rate, absorption, and upper level formation rate is analyzed for rare gas halide lasers. The influence of these effects on laser output irradiance uniformity is significant, and it is shown that the optimum laser design is obtained by a compromise between maximum extraction efficiency and output uniformity. The results are presented in a parametric manner for general applicability.

Published in *Optical Engineering*, Volume 30, No. 3, March 1991.

14. SUBJECT TERMS	15. NUMBER OF PAGES
lasers solid state electro-optics	16. PRICE CODE

17. SECURITY CLASSIFICATION OF REPORT	18. SECURITY CLASSIFICATION OF THIS PAGE	19. SECURITY CLASSIFICATION OF ABSTRACT	20. LIMITATION OF ABSTRACT
UNCLASSIFIED	UNCLASSIFIED	UNCLASSIFIED	SAME AS REPORT

21a. NAME OF RESPONSIBLE INDIVIDUAL	21b. TELEPHONE *(Include Area Code)*	21c. OFFICE SYMBOL
R. Scheps	(619) 553–3730	Code 843

Extraction efficiency uniformity in rare gas halide lasers

Richard Scheps
Naval Ocean Systems Center
Code 843
San Diego, California 92152

Abstract. The dependence of the extraction efficiency on the temporal variations in the quenching rate, absorption, and upper level formation rate is analyzed for rare gas halide lasers. The influence of these effects on laser output irradiance uniformity is significant, and it is shown that the optimum laser design is obtained by a compromise between maximum extraction efficiency and output uniformity. The results are presented in a parametric manner for general applicability.

Subject terms: lasers; excimers; uniformity; extraction efficiency.

Optical Engineering 30(3), 317-322 (March 1991).

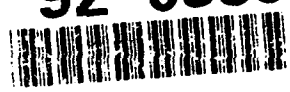

CONTENTS

1. INTRODUCTION

Output irradiance uniformity is a major factor in determining laser design suitability for applications such as Raman conversion[1,2] or optical pumping. The temporal uniformity is sensitive to variations in the extraction efficiency caused by changes in quenching rates that occur during the pulse. These rate changes are due to temperature increases and halogen burn-up and can be significant for electron beam pumping with specific energy loadings on the order of 0.1 J/cm^3. It is therefore important to examine the impact of these changes on the output uniformity. While a detailed discussion of the specific mechanisms that are responsible for temporal variations in the gain and absorption will be presented elsewhere,[11] the model developed here establishes the relationship between irradiance uniformity and medium kinetics. This enables one to determine an acceptable range for parametric variations once a design goal for irradiance uniformity is established. An example of the application of these results is provided for a KrF laser.

Paper 2812 received Oct. 5, 1989; revised manuscript received July 26, 1990; accepted for publication Aug. 7, 1990.

2. MODEL

For a homogeneously broadened laser the output irradiance I_{out} is related to the extraction efficiency η by

$$\eta = \frac{\beta_{out}}{g_0 L}\frac{R - A}{R + Q}, \tag{1}$$

where $\beta_{out} = I_{out}/I_s$ is the normalized output irradiance, g_0 is the unsaturated gain, I_s is the saturation irradiance, L is the length of the gain medium, R is the terminal laser level removal rate, A is the Einstein A coefficient, and Q is the quenching rate. The one-dimensional flux transport model given by Rigrod[3] results in the approximation

$$\beta_{out} \approx \frac{(g_0 - \alpha_0)L + \ln r^{1/2}}{1 - [\alpha_0 L/\ln r^{1/2}]}, \tag{2}$$

where α_0 is the absorption coefficient and r is the reflectivity of the output coupler. Rigrod's model further identifies an optimum output coupling that maximizes both the output irradiance and power extraction efficiency when the other parameters are fixed. (The power extraction efficiency is defined[4] as the ratio of the output intensity to the upper level pump rate.) Since the optimum output coupling is based on specific loss and unsaturated gain values, changes in the gain and absorption during the excitation pulse lead to nonoptimum resonator performance, accompanied by changes in efficiency and irradiance. In the following sections, the dependence of the extraction efficiency on these macroscopic laser parameters is established, and its relationship to the output irradiance uniformity is discussed. Schindler[5] has shown that Rigrod's approximate solution to the flux transport equation is inaccurate for $g_0 L > 10$ when $g_0/\alpha_0 > 1.5$, and

therefore the exact solutions are used to calculate the quantitative results in this paper. However, Rigrod's approximation is used to derive the analytical expressions in the model. For the range of parameters relevant to this work, the difference between the two results is insignificant.

2.1. Dependence of extraction efficiency on pump rate

We begin by considering the extraction efficiency as a function of the pump rate (P), quenching rate, and absorption:

$$\eta = \eta(Q,P,\alpha_0) \ , \tag{3}$$

where the dependence of η on the quenching rate and the upper level pumping rate comes from[6]

$$g_0 = \frac{R - A}{Q + A}\frac{\sigma P}{R} \ , \tag{4}$$

with σ being the stimulated emission cross section. The variation in η is then

$$d\eta = \frac{\partial\eta}{\partial Q}dQ + \frac{\partial\eta}{\partial\alpha_0}d\alpha_0 + \frac{\partial\eta}{\partial P}dP \ . \tag{5}$$

For small changes in the independent variables, Eq. (5) can be linearized (Δ^2 and higher terms dropped), giving

$$\Delta\eta \approx \frac{\partial\eta}{\partial Q}\Delta Q + \frac{\partial\eta}{\partial\alpha_0}\Delta\alpha_0 + \frac{\partial\eta}{\partial P}\Delta P \ . \tag{6}$$

The fractional change in η can then be obtained from Eqs. (1) through (6):

$$\frac{\Delta\eta}{\eta} = \left[\frac{Q(R - A)}{(Q + A)(Q + R)} - \frac{g_0 L}{(g_0 - \alpha_0)L + \ln r^{1/2}}\frac{Q}{Q + A}\right]\frac{\Delta Q}{Q} + \left\{\frac{\gamma}{[\ln r^{1/2}/\alpha_0 L - 1][\ln r^{1/2}/\alpha_0 L + (\gamma - 1)]}\right\}\frac{\Delta\alpha_0}{\alpha_0} + \left[\frac{\alpha_0 L - \ln r^{1/2}}{\ln r^{1/2} + (g_0 - \alpha_0)L}\right]\frac{\Delta P}{P} \ , \tag{7}$$

where $\gamma \equiv g_0/\alpha_0$. As a representative case, a 2 m e-beam-pumped XeCl laser might have the following values: $g_0 L = 5$, $\alpha_0 L = 0.5$, $\gamma = 10$, $r = 0.115$, $Q = 10^8\ s^{-1}$, $A = 9\times 10^7\ s^{-1}$, and $R = 9\times 10^8\ s^{-1}$. Equation (7) then is

$$\frac{\Delta\eta}{\eta} = -0.34\frac{\Delta Q}{Q} - 0.46\frac{\Delta\alpha_0}{\alpha_0} + 0.46\frac{\Delta P}{P} \ . \tag{8}$$

For a maximum acceptable $\Delta\eta/\eta$, two to three times this uniformity in the spatial and temporal variation of Q, α_0, or P could be tolerated. Similarly, the fractional change in the normalized output irradiance β_{out} is

$$\frac{\Delta\beta_{out}}{\beta_{out}} = \frac{Q}{Q + A}\frac{-g_0 L}{(g_0 - \alpha_0)L + \ln r^{1/2}}\frac{\Delta Q}{Q} + \left\{\frac{\gamma}{[\ln r^{1/2}/\alpha_0 L - 1][\ln r^{1/2}/\alpha_0 L + (\gamma - 1)]}\right\}\frac{\Delta\alpha_0}{\alpha_0} + \frac{g_0 L}{(g_0 - \alpha_0)L + \ln r^{1/2}}\frac{\Delta P}{P} \ . \tag{9}$$

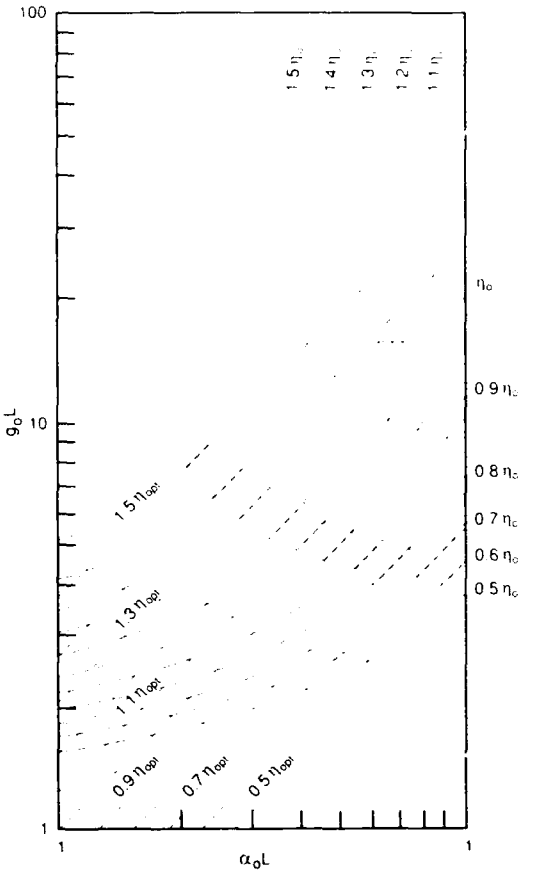

Fig. 1. Curves of constant extraction efficiency (solid lines) indexed to the optimum extraction efficiency ($\eta_{opt} = \eta_0 = 0.47$) at the design point of the resonator: absorption ($\alpha_0 L$) = 0.5, gain ($g_0 L$) = 5, output reflectivity (r) = 0.115. Straight lines (dashed) indicate locus of constant optimum extraction efficiency obtained using Eq. (11) and represent the maximum extraction efficiency one could obtain with optimum output coupling. Constant η_{opt} lines are shown for $\Delta\eta_{opt}$ = 0.1 but labeled for $\Delta\eta_{opt}$ = 0.2.

Comparison of Eqs. (7) and (9) shows that the normalized output irradiance is generally more sensitive to changes in quenching and pump rates than is the extraction efficiency. Evaluating Eq. (9) for the representative case given above results in

$$\frac{\Delta\beta_{out}}{\beta_{out}} = -0.77\frac{\Delta Q}{Q} - 0.46\frac{\Delta\alpha_0}{\alpha_0} + 1.46\frac{\Delta P}{P} \ . \tag{10}$$

While it is desirable to design a laser for optimum extraction efficiency, it has been noted that as g_0 and α_0 change during the pulse, laser operation will proceed in a nonoptimized cavity. In Fig. 1 curves of constant extraction efficiency are shown for a cavity in which the output coupling is optimized at a design point of $g_0 L = 5$, $\alpha_0 L = 0.5$. The curves were obtained by evaluating Schindler's transcendental equation for the cavity flux for the case where $R >> (A + Q)$, and in general they are closely approximated by the Rigrod model. The extraction efficiency for each curve is referenced to the optimum efficiency at the design point ($\eta_0 = 0.47$) with the output reflectivity set at $r = 0.115$. These curves provide a contour map, indicating the direction in which the operational extraction efficiency changes for a given change in $\alpha_0 L$ and $g_0 L$. The infinite gain limit of the constant η curves is determined by the absorption and r, and since in this limit the reflectivity is far off optimum, the efficiency is less than 1.

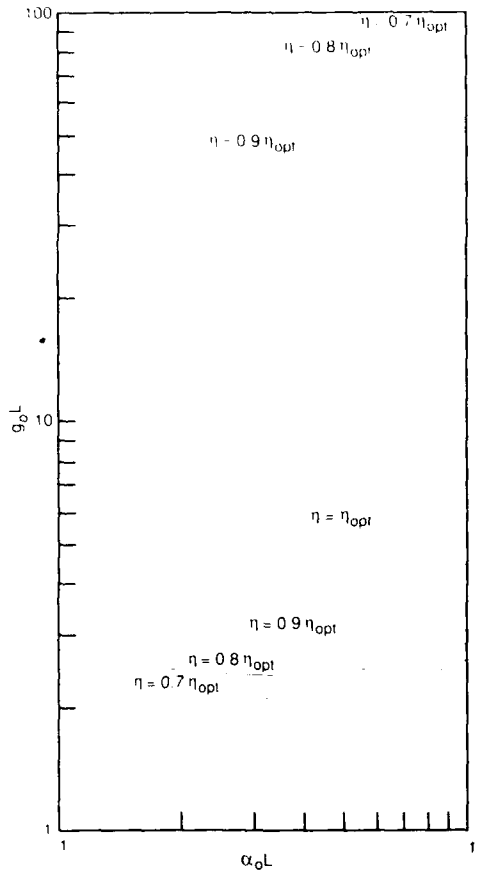

Fig. 2. Deviation of the operational extraction efficiency from the optimum extraction efficiency. The curves of constant *ratio of* η/η_{opt} show the reduction in efficiency obtained by fixing $r = 0.115$ compared with the efficiency one could obtain by optimizing r for each α_0L, g_0L coordinate.

2.2. Optimum extraction efficiency

As the gain and absorption change in time, the extraction efficiency drifts below the optimum extraction efficiency that one could obtain if r were not fixed. Rigrod's approximation expresses the optimum extraction efficiency as

$$\eta_{opt} = (1 - \gamma^{1/2})^2 . \tag{11}$$

and from this equation it can be seen that η_{opt} will vary slowly with changes in gain and absorption. Figure 1 shows several lines of constant optimum extraction efficiency, indexed to the optimum efficiency at the design point. The intersection of the constant η curves with the η_{opt} lines yields the ratio of operational to optimum extraction efficiency at the intersection point and therefore provides a measure of the loss in efficiency when the cavity is operated at the intersection point (α_0L, g_0L) and an output reflectivity of 0.115. Figure 2 shows curves of constant η/η_{opt} plotted in α_0L, g_0L coordinates. These curves were obtained for the design point of Fig. 1. For efficiency ratios other than 1, two "branches" are obtained, representing cases where the fixed output coupling is either too high or too low (two intersection points in Fig. 1). The broad range of α_0L, g_0L values for which $\eta > 0.9\,\eta_{opt}$ indicates that small changes in the coordinates will not greatly reduce the extraction efficiency below its optimum value, even though its absolute value may vary considerably.

2.3. Irradiance uniformity

As was mentioned in discussing Eq. (9), the normalized output irradiance is more sensitive to changes in gain than is the extraction efficiency. The saturation irradiance is constant only if the quenching rates are constant, in which case $\Delta\beta_{out} = \Delta I_{out}$. If quenching of the upper level is not constant,

$$\frac{\Delta I_{out}}{I_{out}} = \frac{\Delta I_s}{I_s} + \frac{\Delta\beta_{out}}{\beta_{out}} . \tag{12}$$

The variation in output irradiance about the design point is shown graphically in Fig. 3. Note that for this figure, as well as for Figs. 1 and 2, the range of variation in g_0L and α_0L shown in the curves is greater than can be justified by the linearization approximation. However, it can be clearly seen that small changes in the gain and absorption produce even greater changes in the output irradiance than in the extraction efficiency. At the design point the output irradiance is $2.34I_s$.

3. NUMERICAL EXAMPLE AND IMPLICATIONS FOR LASER DESIGN

To demonstrate the application of the model developed in the previous section, we consider an e-beam-pumped KrF laser excited by a 500 ns pulse in an Ar/Kr/F_2 mixture, pumped with a specific energy loading of 0.1 J/cm^3. The change in the gain comes primarily from two phenomena that independently affect the quenching rates. The first is the gas heating, which affects the rate coefficients, and the second is the fluorine depletion, which both increases the electron density and hence the electron quenching rate, and reduces the halogen quenching rate. Using published values for the temperature dependence of the three body quenching rate coefficient,[7] the attachment rate coefficient,[8] the electron quenching rate,[9] and the halogen quenching rate,[10] combined with the dependence of the fluorine depletion rate on the pump rate,[9] one can obtain $g_0(t)$. The details of this calculation will be presented elsewhere.[11] The magnitude of the temperature-induced changes depends on the argon density, while the initial fluorine density determines the influence of fluorine depletion. A range of conditions can therefore be identified under which these changes are minimized.

With a fixed ratio of $[F_2]:[Ar] = 1.7 \times 10^{-3}$, $\Delta g_0L/g_0L$ is 0.10 at 1.5 amagat argon and 0.20 at 2 amagat. These argon densities keep the variation in g_0 low, and for both densities the change represents the gain increasing from its initial value. The absorption change during the pulse is due primarily to fluorine depletion since the other major absorbers (F^- and Kr_2F^*) do not undergo significant density changes. The decrease in net absorption, $\Delta\alpha_0L/\alpha_0L$, is a little over 0.1 for both argon densities considered. From Fig. 1 it can be seen that under these conditions the fractional change in the extraction efficiency is 0.10 and 0.15, while Fig. 3 shows that the change in the normalized output irradiance is 0.2 and 0.35 for the 1.5 amagat and 2 amagat mixtures, respectively.

While these changes are significant, shorter pulse lengths and lower $[F_2]:[Ar]$ ratios give rise to even larger nonuniformities. The sensitivity of the output irradiance to changes in the gain and absorption shown in Fig. 3 indicates that some care must be taken to consider irradiance uniformity when designing a laser around a given operating point. This is especially true for lasers where the internal flux is large since temporal increases in output irradiance can exceed the threshold for optical damage to the

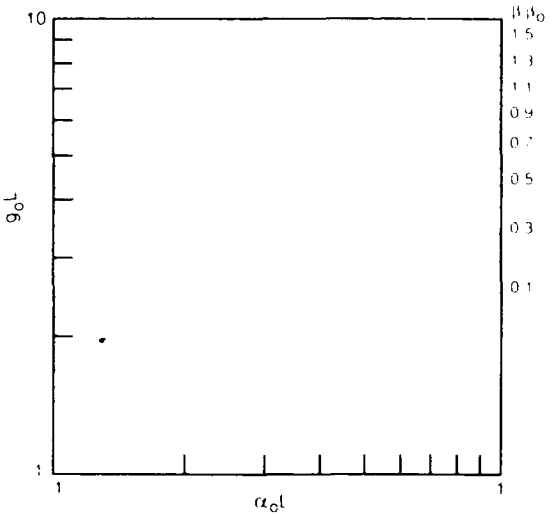

Fig. 3. Curves of constant normalized output irradiance indexed to the normalized output irradiance at the design point of Fig. 1 ($\beta_0 = 2.34/_s$). Constant β/β_0 curves are shown for $\Delta(\beta/\beta_0) = 0.1$ but labeled for $\Delta(\beta/\beta_0) = 0.2$.

optical elements. On the other hand, damage can be avoided if optics are sized for peak irradiance, but significant cost inefficiencies will result if the optical elements are large. The key to optimizing laser performance for irradiance uniformity (assuming uniform energy deposition) is in selecting the resonator design point in such a manner as to minimize the effects of anticipated g_0 and α_0 changes. In general, this will require selecting an output coupling that is higher than optimum so that the improved uniformity is obtained by compromising the magnitude of the output irradiance. One must therefore consider trading off extraction efficiency magnitude for extraction efficiency uniformity, or equivalently, output energy for output uniformity.

4. CONCLUSIONS

For the 500 ns e-beam-pumped KrF laser described, the magnitude of the normalized output irradiance uniformity will lie in the 20% to 35% range. This might be unacceptable for a nonlinear Raman conversion process, for example, but lasers designed for other applications may have much larger tolerances for variations. It would be useful to compare the nonuniformities obtained from the kinetics considerations in this work with temporal and spatial nonuniformities expected from phenomena such as nonuniform e-beam deposition and transverse amplified spontaneous emission (ASE). E-beam-pumped excimer lasers vary greatly in size and intended use, however, and the nonuniformities inherent in demonstrated designs cover an extremely wide range. For example, the large "Scale-Up" excimer laser designed by AVCO[12] displayed temporal variations in e-beam current that were typically 300% over 2 μs, although an e-beam-pumped device designed by AVCO for Raman conversion* provided much more uniform output. Short pulse operation can avoid temporal e-beam current variations by staying well below the diode closure time, but kinetics-driven nonuniformities in short pulse systems are more severe.[11]

It is not practical to present quantitative estimates of the nonuniformities arising from all possible sources, but within the context of the present calculations (which allow one to "fine-tune" a laser that has already been designed for output uniformity) we examine several excimer laser designs in which output uniformity is a consideration. The direct relationship between pumping uniformity and variations in the output flux were established in Sec. 2, but the most obvious source of pump nonuniformity is the variation in temporal and spatial energy deposition of the e-beam. Optical beam quality measurements using a Mach-Zender interferometer have been shown[13,14] to provide direct information on the spatial variation of the e-beam deposition profile through a determination of the transient refractive index. The XeF laser in Ref. 14 produced a peak phase shift of 5 rad over 2 m and a variation in ion pair production rate of 4% over a 5 cm aperture. A much improved 1 m XeF laser designed for high beam quality was recently reported[15] to produce near-diffraction-limited output with a Strehl ratio of 0.76 throughout a 500 ns pulse. Modeling of a large scale KrF laser[16] for laser fusion indicates that with two-sided pumping, diode impedance collapse requires a tradeoff between spatial and temporal e-beam energy deposition uniformity. For example, the spatial deposition uniformity can be maintained within 10% across a 1 m aperture, but under these conditions the temporal variation in pump rate during a 1 μs pulse exceeds 40%.

Another major contribution to spatial nonuniformity, particularly for large aperture devices, is the transverse ASE.[17,18] For apertures of several centimeters this effect is negligible, but beyond 50 cm the transverse ASE flux becomes an important factor in determining output uniformity. This comes about due to the nonuniform flux profile, which is largest at the aperture edge and causes nonuniform gain across the aperture. For a 3 m long by 1 m square-aperture KrF laser with a g_0 of 0.04/cm, the transverse ASE nonuniformity[18] will be 20%. Nonuniformities can also result from the extraction dynamics of the unstable resonator. This occurs since a fraction of the laser volume sees only one pass of the extracting flux while other parts of the volume see two or more. This "picture frame" effect leads to spatial nonuniformities on the order of 20%. A related phenomenon arises from the competition between the intracavity coherent flux and longitudinal ASE. This competition is affected by the resonator output coupling because a large longitudinal ASE flux can develop if the coherent flux fails to saturate the gain. Since the spatial variation of the intracavity flux resulting from the picture frame effect can lead to unloaded gain regions within the active volume, additional output nonuniformities will arise.

In conclusion, it has been shown that small changes in the gain and absorption may lead to substantial changes in the laser output irradiance. Changes in the kinetics rates and species densities that occur during the excitation pulse are a result of gas heating and halogen donor removal, and these variations may cause unacceptable changes in output irradiance in a poorly designed rare gas halide laser. The temporal irradiance nonuniformities will occur even though the pumping is both temporally and spatially uniform and can be restricted in magnitude by suitable selection of gas mixture, total pressure, and pulse length.

5. APPENDIX: OPTIMUM EXTRACTION EFFICIENCY

Equation (11) is obtained directly from Rigrod's[3] model for volumetric extraction efficiency, but the optimum local extraction efficiency for an infinitesimal slab of gain medium in a single pass amplifier[6] is given by the same expression. This is

*M. J. Boness, private communication.

contrary to what one might expect since the optimum extraction efficiency for the finite length gain medium should differ from that for the infinitesimal slab due to the axial (z) dependence of the intracavity flux. This section is directed toward demonstrating that the equivalence of the calculated optimum extraction efficiency for the two gain lengths is a direct consequence of the average gain approximation in the Rigrod model and as such puts a limitation on the application of Eq. (11) to an actual laser. The Rigrod solution for the lossy traveling wave resonator is considered here since the analogy to the single pass amplifier is most direct. However, the conclusions are valid for the standing wave resonator as well.

The saturated gain along the z axis in the active medium can be written as

$$\frac{d\beta}{dz} = \frac{g_0\beta}{1+\beta} - \alpha_0\beta \ , \tag{13}$$

where β is the interior irradiance normalized to the saturation irradiance. Equation (13) is appropriate when ground state dissociation is rapid. For the infinitesimal gain slab the optimum extracting flux β_{max} can be found directly by differentiating Eq. (13) with respect to β and setting the derivative equal to zero. This gives

$$\beta_{max} = \gamma^{1/2} - 1 \ , \tag{14}$$

from which Eq. (11) follows since

$$\eta_{local} = \frac{1}{g_0}\frac{d\beta}{dz} \ . \tag{15}$$

The finite length optimum irradiance can be found by integrating Eq. (13),

$$\int_{\beta}^{\beta+\Delta\beta} (1+\beta^{-1})d\beta = \int_0^{\Delta z} (g_0 - \alpha_0 - \alpha_0\beta)dz \ , \tag{16}$$

where $\Delta\beta$ is the increase in the irradiance for a single pass through the gain medium and Δz is the gain length, to obtain

$$\Delta\beta + \ln\left(1+\frac{\Delta\beta}{\beta}\right) = (g_0 - \alpha_0)\Delta z - \int_0^{\Delta z}\alpha_0\beta dz \ . \tag{17}$$

Defining the average irradiance as

$$\bar{\beta} \equiv \frac{\int_0^{\Delta z}\beta(z)dz}{\int_0^{\Delta z}dz} \ , \tag{18}$$

Eq. (17) becomes

$$\Delta\beta + \ln\left(1+\frac{\Delta\beta}{\beta}\right) = (g_0 - \alpha_0)\Delta z - \alpha_0\bar{\beta}\Delta z \ . \tag{19}$$

To obtain an analytical solution to Eq. (13), Rigrod defines the average gain $\bar{g}$ as

$$\bar{g} = \frac{g_0}{1+\bar{\beta}} - \alpha_0 \tag{20}$$

and approximates the solution to $\beta(z)$ as

$$\beta(z) = \beta_{in}\exp(\bar{g}z) \ , \tag{21}$$

where β_{in} is the irradiance at $z = 0$. Equations (18) and (21) then lead to

$$\ln\left(1+\frac{\Delta\beta}{\beta}\right) = \frac{\Delta\beta}{\bar{\beta}} \ , \tag{22}$$

with $1 + \Delta\beta/\beta = \exp(\bar{g}\Delta z)$ and $\beta = \beta_{in}$. Rewriting Eq. (19), one obtains

$$\frac{\Delta\beta}{\Delta z} = \bar{\beta}\left(\frac{g_0}{1+\bar{\beta}} - \alpha_0\right) = \bar{\beta}\bar{g} \ . \tag{23}$$

Maximizing $\Delta\beta/\Delta z$ with respect to $\bar{\beta}$ produces the equivalent of Eq. (14) for $\bar{\beta}$, and since $\eta = \Delta\beta(g_0\Delta z)^{-1}$, η_{opt} for the finite length laser is also given by Eq. (11).

The impact of the average gain approximation can be clearly resolved by defining the average extraction efficiency as

$$\bar{\eta} = \frac{\int_0^{\Delta z}\eta_{local}(z)dz}{\Delta z} = \frac{1}{g_0\Delta z}\int_0^{\Delta z} d\beta = \frac{1}{g_0}\frac{\Delta\beta}{\Delta z} = \frac{1}{g_0}\bar{\beta}\bar{g} \ . \tag{24}$$

Comparison of Eq. (24) with Eq. (15) shows that the Rigrod model calculates the analog of the thin slab local efficiency for an extracting flux intensity equal to $\bar{\beta}$ and medium saturated amplification factor $\bar{g}$. While the medium as modeled does not approximate a thin slab [$\ln(1 + \Delta\beta/\beta) \neq \Delta\beta/\beta$ and $\bar{\beta} \neq \beta$], it is important to note that only the $\bar{g}$ approximation requires small axial variations in the cavity flux.

In the context of the previous analysis, it can be shown that the fit to Eq. (11) obtained by Chernin[6] for the extraction efficiency in a confocal unstable resonator results from the range of cavity parameters he selected. Based on reasonable expectations for rare gas halide lasers, g_0L was kept below 10. This kept the intracavity flux variations low and the average gain approximation therefore applied. In such an instance the optimum volumetric extraction efficiency will be given by Eq. (11).

Near the optimum flux, the thin slab extraction efficiency is insensitive to small changes in the interior irradiance associated with flux propagation through the cavity. An expression relating the change in extraction efficiency to the interior irradiance can be obtained from Eqs. (13) and (15):

$$\eta_{local} = \frac{\beta}{1+\beta} - \frac{\beta}{\gamma} \ . \tag{25}$$

Combining this with Eqs. (11) and (14) gives

$$\frac{\Delta\eta}{\eta_{opt}} = \frac{(1-\omega)^2}{1-\omega(1-\gamma^{1/2})} \ , \tag{26}$$

where $\beta = \omega\beta_{max}$ and $\Delta\eta = \eta_{opt} - \eta$. For $\gamma = 10$, a 20% change in β ($\omega = 0.8$) produces only a 1% change in η, while a 50% change in β causes η to decrease by 12%.

6. REFERENCES

1. A. Flusberg and D. Kortt, "Transient refractive index changes in stimulated Raman scattering," JOSA B3(10), 1338–1344 (1986).
2. R. T. V. Kung, "Nonlinear index effects due to pump laser bandwidth in Raman conversion," IEEE J. Quantum Electron. QE-18(12), 2056–2059 (1982).
3. W. W. Rigrod, "Homogeneously broadened cw lasers with uniform distributed loss," IEEE J. Quantum Electron. QE-14(5), 377–381 (1978).
4. A. E. Siegman, *Lasers*, pp. 485–489, University Science Books, Mill Valley, Calif. (1986).
5. G. M. Schindler, "Optimum output efficiency of homogeneously broadened lasers with constant loss," IEEE J. Quantum Electron. QE-16(5), 546–549 (1980).
6. D. P. Chernin, "Optical extraction efficiency in lasers with high Fresnel number confocal unstable resonators," Appl. Opt. 18(21), 3562–3566 (1979).
7. V. H. Shui, "Temperature dependence of recombination rate constants for $KrF^* + R + R \rightarrow RKrF^* + R(R = Ar,Kr)$," Appl. Phys. Lett. 34(3), 203–204 (1979).
8. M. Rokni, J. A. Mangano, J. H. Jacob, and J. C. Hsia, "Rare gas fluoride lasers," IEEE J. Quantum Electron. QE-14(7), 464–481 (1978).
9. D. W. Trainor, "Short pulse KrF kinetics," in *Advanced Laser Meeting, Session IV(A)—Angular Optical Multiplexing I*, W. J. Schafer Associates, Inc., Rept. No. WJSA 78-6 SR-13A, pp. TR-01–TR-53 (1979).
10. J. G. Eden, R. S. F. Chang, and L. J. Palumbo, "Absorption in the near ultraviolet wing of the Kr_2F^* (410 nm) band," IEEE J. Quantum Electron. QE-15(10), 1146–1156 (1979).
11. R. Scheps, "Output irradiance uniformity in a single pass KrF amplifier," Opt. Laser Technol., 22(6), 387–393 (1990).
12. L. Litzenberger, M. J. Smith, and D. Trainor, "Excimer laser performance studies," Final Rept. Vol. II, No. N00014-84-C-0629 ARPA No. 9031 (1987).
13. R. Scheps, R. O. Hunter, and J. R. Oldenettel, "Interferometric technique for transient phase shift measurements in an electron-beam-pumped laser," Rev. Sci. Instrum. 50(9), 1054–1061 (1979).
14. R. Scheps, "Phase shift measurements in electron-beam pumped XeI," Opt. Eng. 28(9), 969–974 (1989).
15. C. Londono, M. J. Smith, D. W. Trainor, R. Berggren, S. F. Fulgham, and I. Itzkan, "Detailed optical characterization of a near diffraction limited xenon fluoride laser," IEEE J. Quantum Electron. 24(12), 2467–2476 (1988).
16. G. R. Allen, L. A. Rosocha, M. Kang, and E. M. Honig, "Electron-beam pumping technology for KrF lasers," in *Inertial Confinement Fusion at Los Alamos, Vol. I*, D. C. Cartwright, ed., Chap. VII, pp. 1–8, Los Alamos Rept. No. LA-UR-89-2675 (1989).
17. A. M. Hunter and R. O. Hunter, "Bidirectional amplification with nonsaturable absorption and amplified spontaneous emission," IEEE J. Quantum Electron. QE-17(9), 1879–1887 (1981).
18. A. M. Hunter, R. O. Hunter, and T. H. Johnson, "Scaling of KrF lasers for inertial confinement fusion," IEEE J. Quantum Electron. QE-22(3), 386–404 (1986).

Richard Scheps received his Ph.D. from the University of Chicago in chemical physics and received his BS degree from the University of California at Berkeley. He has been actively involved in laser research since 1973 and has published numerous papers in this field and presented his results at major conferences. After completing his graduate studies, Dr. Scheps was awarded a postdoctoral fellowship at the Joint Institute for Laboratory Astrophysics in Boulder, Colo. He had held several senior positions in corporate laser research before joining the Naval Ocean Systems Center. He has been involved in the management of the XeCl laser submarine communications program and also heads an active experimental research program in diode-pumped solid-state lasers.